Palaeogeography, Palaeoclimatology, Palaeoecology 577 (2021) 110535

Contents lists available at ScienceDirect

Palaeogeography, Palaeoclimatology, Palaeoecology

journal homepage: www.elsevier.com/locate/palaeo

Temperature, precipitation, and vegetation changes in the Eastern Mediterranean over the last deglaciation and Dansgaard-Oeschger events

Mona Stockhecke [a,b,c,*], Achim Bechtel [d], Francien Peterse [e], Typhaine Guillemot [f], Carsten J. Schubert [f,g]

[a] Department of Surface Waters-Research and Management, EAWAG, Überlandstr. 133, 8600 Dübendorf, Switzerland
[b] University of Minnesota Duluth, Large Lake Observatory, Duluth, MN 55812, USA
[c] Geological Institute, ETH Zürich, Sonneggstr. 5, 8092 Zürich, Switzerland
[d] Department of Applied Geosciences & Geophysics, Montanuniversität Leoben, Peter-Tunner-Str. 5, A-8700 Leoben, Austria
[e] Department of Earth Sciences, Utrecht University, Princetonlaan 8A, 3584, CB, Utrecht, the Netherlands
[f] Department of Surface Waters-Research and Management, EAWAG, Seestr. 79, CH-6047 Kastanienbaum, Switzerland
[g] Department of Environmental Systems Science, ETH Zürich, Universitätstrasse 16, 8092 Zürich, Switzerland

ARTICLE INFO

Editor: Shucheng Xie

Keywords:
Biomarkers
C-isotopes
H-isotopes
Glycerol dialkyl glycerol tetraethers
Precipitation

ABSTRACT

We here estimate past temperature and hydroclimate variations in eastern Anatolia for marine isotope stages 4 to 1 (MIS4 to MIS1) respectively using branched glycerol dialkyl glycerol tetraethers (brGDGTs) and the hydrogen isotopic composition of *n*-C_{29} leaf-wax *n*-alkanes (δ^2H_{wax}) stored in the sedimentary record of Lake Van (Turkey). Our millennial-scale lipid biomarker records reflect warm and wet conditions during interstadials/interglacials and colder and dryer periods with increased evapotranspiration and aridity during stadials/glacials. The degree of methylation of the 5-methyl brGDGTs (MBT'_{5me}) indicates increasing mean annual air temperatures (MAT) during stadial/interstadial transitions, that characterize Dansgaard-Oeschger events, and during the last glacial termination.

Based on the effects of changes in precipitation amount on apparent enrichment factors between the δ^2H of the C_{29} *n*-alkanes and δ^2H of precipitation, a total increase in annual precipitation of about 200 mm during transitions from stadials to interstadials, and of 300–350 mm during glacial-interglacial transitions can be determined, in line with previous paleoclimate reconstructions for the Eastern Mediterranean.

High sterol concentrations in sediments deposited during warm and humid interstadials reflect increases in lake level, vegetation density and algal blooms, whereas lower values of the branched versus isoprenoid tetraethers ratio (BIT) likely reflects the increased niche of Thaumarchaeota resulting from enhanced windiness and mixing of the water column during colder periods. This quantitative hydroclimate reconstruction from Lake Van (Turkey), as it is optimally situated to respond to North Atlantic climate change via changes in the large-scale wind fields shed light into millennial-scale global climate variability.

1. Introduction

Information about the magnitude of temperature and precipitation changes during the last glacial termination and within the Holocene, as well as Marine Isotope Stage 3 (MIS3) is scarce for the continental Eastern Mediterranean. Paleoclimatic reconstructions covering several glacial/interglacial cycles in the Eastern Mediterranean are mostly based on marine records from around the Mediterranean Sea (Emeis et al., 2003; Martrat et al., 2004) or continental records from lakes, palynomorphs and speleothems (Tzerdakis et al., 2006; Djamali et al., 2008; Badertscher et al., 2011; Gasse et al., 2011; Francke et al., 2015). The sea surface temperature (SST) of the Black Sea changed with 2–3 °C during stadial/interstadial transitions (20–65 kyr BP; Wegwerth et al., 2015) based on the TEX_{86}, a temperature proxy based on changes in the relative abundance of isoprenoid glycerol dialkyl glycerol tetraether (GDGT) membrane lipids produced by temperature-sensitive archaea in the water column (Schouten et al., 2002). In another study from the Dead Sea, temperature and precipitation changes during the Holocene

* Corresponding author at: Department of Surface Waters-Research and Management, EAWAG, Überlandstr. 133, 8600 Dübendorf, Switzerland.
E-mail addresses: Mona.Stockhecke@eawag.ch (M. Stockhecke), F.Peterse@uu.nl (F. Peterse), Typhaine.Guillemot@eawag.ch (T. Guillemot), Carsten.Schubert@eawag.ch (C.J. Schubert).

https://doi.org/10.1016/j.palaeo.2021.110535
Received 6 January 2021; Received in revised form 15 June 2021; Accepted 16 June 2021
Available online 22 June 2021

were estimated to be in the order of 4–5 °C and up to 150 mm/year, respectively, based on pollen (Litt et al., 2012).

Lake sediments are considered important terrestrial archives of past climate change, especially in areas where other high-resolution records, such as ice cores, are not available. For this reason, the sediments from the endorheic Lake Van (Turkey) were drilled in 2010 within the International Continental Scientific Drilling project (ICDP) Paleovan (Litt and Anselmetti, 2014). Due to its hydrologically closed nature, water level fluctuations reflect the precipitation to evaporation (p/e) ratio in the area (Randlett et al., 2017). Variations in lake productivity, lake level, water mixing and shoreline distance, as well as vegetation changes in correspondence to millennial-scale hydroclimatic variability in the Near East during the last 15 marine isotope stages, have been reconstructed (Stockhecke et al., 2014a). The results of high-resolution studies over the last 600 kyr, including sedimentological and bulk geochemical data, pollen counts and isotopic measurements on carbonates, argue for generally cold and dry conditions during glacials, whereas interglacials were warmer and wetter (Kwiecien et al., 2014; Litt et al., 2014; Stockhecke et al., 2014b). Comparison of the results from the color index B* reflectance of the sediments with model simulations indicates that lake-level rise during interstadials over the last 350 kyr was a result of increased precipitation coupled to the strengthening of the Atlantic Meridional Overturning Circulation (AMOC) (Stockhecke et al., 2016). Studies using lipid biomarkers, which are source or environment-specific organic molecules, preserved in Lake Van sediments provided first insights into long-term environmental changes in the past (Randlett et al., 2014). For example, the occurrence of deuterium (^{2}H)-enriched C_{29} *n*-alkanes and C_{37} alkenones during MIS4 and MIS2 point towards dry climate conditions in the Lake Van region at this time, which was attributed to a decrease in the regional p/e ratio during this period, and independently supported by a maximum in pore water salinity (Randlett et al., 2017; Tomonaga et al., 2017).

However, information about the timing and relative magnitude of changes in temperature and hydroclimate is still missing on millennial timescales. Therefore, we here study sediment samples from Lake Van, covering the time interval from the onset of MIS4 to present (0–70 kyr). Two intervals from Last Glacial Maximum up to present (0–22 kyr) and during MIS3 (42–55 kyr), were selected to assess (hydro)climatic and ecological changes at sub millennial-scale. We use down-core distributional changes in branched glycerol dialkyl glycerol tetraethers (brGDGTs), which are membrane lipids of temperature-sensitive bacteria, in combination with the leaf wax hydrogen isotopic composition (δ^2H_{C29}) to respectively reconstruct the relative changes in regional air temperature and the sources of meteoric water during stadial/interstadial transitions as well as the last deglaciation. The effect of evapotranspiration on δ^2H is evaluated by additionally analyzing short- (*n*-$C_{18:0}$) and long-chain (*n*-$C_{28:0}$) saturated fatty acids representing a lacustrine (algal) vs terrestrial (higher plant) signal, respectively. Furthermore, plant-derived lipid biomarkers (*n*-alkanes, sterols) were extracted at centennial resolution to gain insight into the response of vegetation and algal communities on climate change and compared with changes in the branched and isoprenoid tetraether (BIT) index as an indicator of water column conditions. The multi-proxy records allow for the assessment of the magnitude and relative timing of humidity and temperature variations over this period.

2. Setting

Lake Van is located on the eastern Anatolian high plateau (Turkey, 38.5°N, 43°E, 1648 m a.s.l.). The Lake Van catchment covers a surface of 16,000 km^2 (Degens and Kurtman, 1978) and the lake-levels follow precipitation changes rather than evaporation (Stockhecke et al., 2016). With a volume of 607 km^3, Lake Van is considered as the fourth largest terminal lake and the largest soda lake in the world. Its lake waters are highly alkaline, reaching a pH of 9.8 and a salinity of 22 psu. At approximately 539 ka, likely a tectonic event isolated the lake, making it endorheic. Since this period, the local p/e ratio is reflected by the water level of the lake (Stockhecke et al., 2014b), except for several periods of water level high stands (e.g. during MIS7 and MIS5e; North et al., 2017, Tomonaga et al., 2017, Stockhecke et al., 2014b) causing overflow of the lake. The water column undergoes seasonal stratification with epilimnic temperatures reaching up to 25 °C. Annual water mixing during the cold season affects the uppermost 70 m only and thus deep-water temperatures are constant at ~3.3 °C (Stockhecke et al., 2012).

A semi-annual cycle in precipitation is a characteristic feature of high-elevation regions in the East Mediterranean. The south-easterly winds that dominate in spring transport moisture from the Caspian or Arabian Sea into the area, while south-westerly winds bring moisture from the Mediterranean Sea during fall (Stockhecke et al., 2016). Summer aridity results from largescale subtropical subsidence caused by the interaction of the mid-latitude Westerlies and the Asian Monsoon (Rodwell and Hoskins, 1996). Anomalously dry (wet) years are typically related to anomalous high (low) sea level pressure over the North Atlantic (from 45° latitude northward) and the Eastern Mediterranean. These sea level pressure anomalies promote northerly (southerly) winds over Turkey (Eshel and Farrell, 2000). It shows a direct linkage between North Atlantic climate variability and hydroclimatic shifts in the Eastern Mediterranean.

Under present-day conditions, precipitation peaks in April and in October/November, with a warm and dry summer and a cold and intermediately wet winter season separating the two rainy seasons. The strong seasonality is expressed as cold winters from December to February with mean temperatures below 0 °C, and warm summers in July and August with mean temperatures exceeding 20 °C (Stockhecke et al., 2012).

The recent vegetation around the lake is characterized by xeromorphic step vegetation. In the research area, herbaceous formations with step characteristic are the predominant vegetation type (Ozturk and Erkan, 2010). Due to a strong gradient in annual precipitation, the vegetation in the northeastern region is characterized by high plateau steppe and oak-forest remnants, whereas the southwestern region is characterized by a Kurdo-Zagrosian oak forest (van Zeist and Woldring, 1978; Wick et al., 2003).

3. Material and methods

3.1. Lithology and chronology of the sedimentary record

A 219 m long sediment core was drilled at Ahlat Ridge (AR; Fig. 1) (ICDP Site 5034–2, 38.667°N, 42.669°E) at a water depth of 350 m in summer 2010 (Litt and Anselmetti, 2014). The lithostratigraphy of the core from Holocene to MIS4 is characterized by laminated and banded clayey silts, interrupted by volcaniclastic layers and turbidites. The lithological successions are reflected by variations in total organic carbon (TOC) and calcium carbonate content ($CaCO_3$). TOC-rich varved (annually-laminated) clayey silts correspond with rising lake levels (in association with a large anoxic deep water body) deposited during the interglacials, while TOC-poor banded and mottled clayey silts (in association to an oxygenated hypolimnion) are deposited as a consequence of lake-level lowering during the glacials (Stockhecke et al., 2014b).

The entire sedimentary column from the Ahlat Ridge covers approximately the past 600,000 years or MIS 1–15 (Stockhecke et al., 2014a). The age model was constructed using climatostratigraphic alignment, varve chronology, tephrostratigraphy, argon-argon single-crystal dating, radiocarbon dating, magnetostratigraphy, and cosmogenic nuclides (Stockhecke et al., 2014a, 2016). The period from present to 12 ka is based on age constrains from two radiocarbon ^{14}C ages and four marker layers from a varve chronology. From 12 to 70 ka one radiocarbon ^{14}C age and alignment of the B* reflectance to NGRIP GICC05 (Andersen et al., 2004; Rasmusssen et al., 2006; Svensson et al., 2008; Blockley et al., 2012) were used. This is confirmed by the identification of the Laschamp event (Vigliotti et al., 2014; Lachner et al.,

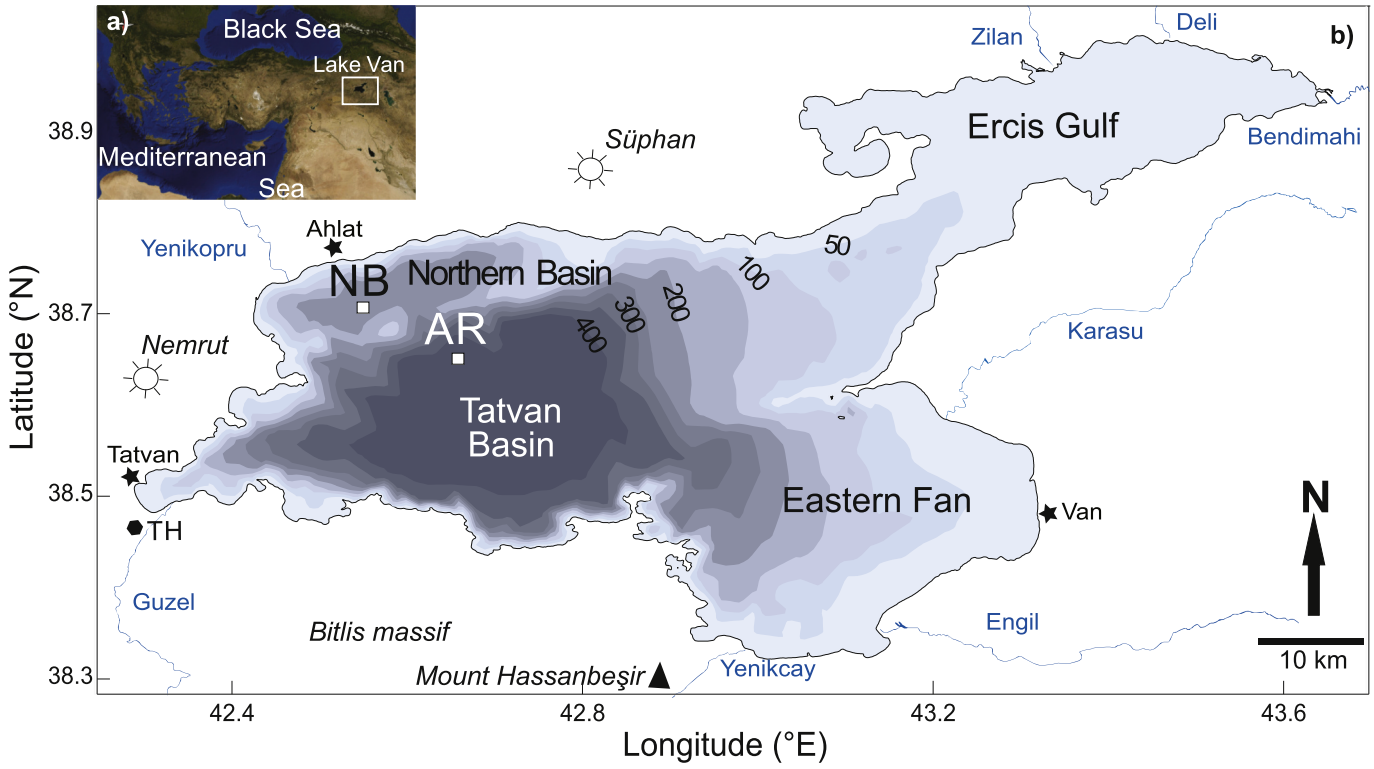

Fig. 1. (a) Map of Eastern Anatolia and location of Lake Van in Turkey, as well as (b) bathymetric map with drilling location Ahlat Ridge (AR).

2021), two tephrostratigraphy marker layers (Stockhecke et al., 2014b) and two radiometric $^{40}Ar/^{39}Ar$ ages (Engelhardt et al., 2017). The given error including 200 year-uncertainties from alignment of the age model for the last 15 kyr is below 400 years, from 15 to 30 kyr it is maximal 1000 years respective between 900 and 1600 years for 42 to 70 kyr. Further details can be found in Stockhecke et al. (2016).

3.2. Lipid extraction and purification

A total of 110 samples from the upper 33 m from the sediment core was selected for lipid analysis and compound-specific isotope analyses, including three samples from the short gravity core to cover the Holocene (Fig. 2). All samples were freeze-dried and homogenized before lipid extraction.

An internal standard composed of known amounts of 5α-cholestane, C_{19} *n*-alkanol, and $C_{19:0}$ *n*-fatty acid (FA), was added to 1–4 g of dry sediment prior to the extraction process. Lipids were extracted with 10 mL of a mixture of dichloromethane (DCM) and methanol (MeOH) (7:3 *v*/v) in microwave Teflon bombs, following a program of 2 min (min) at 300 watts (W) and 5 min at 500 W. The total lipid extract (TLE) was transferred to a separatory funnel containing 20 mL of nanopure water (H_2O) with 5% sodium chloride (NaCl) to remove the salts from the sample. Lipids were extracted from the saline aqueous phase using 3 × 10 mL DCM. Fatty acids (FAs) were released by saponification in approximately 3 mL of 6% potassium hydroxide (KOH) solution in MeOH at 80 °C for 3 h. Neutral lipids were extracted from the KOH/MeOH solution using 3 × 1 mL *n*-hexane, and then separated over a silica column (230–400 mesh Merck, 4 cm length, 0.6 cm diameter) into 3 fractions of various polarity using 4 mL of the following eluents: 1) *n*-hexane:DCM (9:1 *v*/v); 2) *n*-hexane:DCM mixture (1:1 v/v) and 3) DCM:MeOH mixture (1:1 v/v). The apolar fraction contained the long-chain *n*-alkanes and the polar (third) fraction contained the sterols and GDGTs. The FAs were recovered from the KOH/MeOH solution with 3 × 1 mL *n*-hexane after acidification to pH = 1. After recovery, the FAs were transformed into methyl esters (FAMEs) by treating them with BF_3/MeOH at 80 °C for 2 h and subsequent extraction with 3 × 1 mL *n*-hexane.

3.3. Lipid biomarker analysis

The *n*-alkanes, sterols, and FAMEs were quantified by gas chromatography – flame ionization detection (GC-2010Plus, Shimazdu, Kyoto, Japan). Samples were injected by an AOC-20i autosampler (Shimadzu) through a split/splitless injector operated in splitless mode at 280 °C. The GC column was an InertCap 5MS/NP (0.25 mm × 30 m × 0.25 μm) (GL Sciences, Japan). It was heated from 70 °C to 130 °C at 20 °C/min, then to 320 °C at 4 °C/min, held at 320 °C for 20 min. The different biomarkers were identified by gas chromatography – mass spectrometry (GCMS-QP2010 Ultra, Shimadzu) under the same analytical conditions. The *n*-alkanes and sterols were quantified using the peak areas relative to those of the respective internal standard (5α-cholestane and C_{19} *n*-alkanol), normalized to TOC.

A known amount of C_{46} GTGT standard was added to the third fraction, containing the GDGTs (Huguet et al., 2006). The fraction was dissolved in an *n*-hexane: isopropanol mixture (99:1, *v*/v), and filtered over a 0.45 μm PTFE filter prior to analysis using high performance liquid chromatography/atmospheric pressure chemical ionization-mass spectrometry (HPLC/APCI-MS) on an Agilent 1260 Infinity series HPLC coupled to an Agilent 6130 single quadrupole mass detector with instrument settings according to Hopmans et al., (2016), Separation of different GDGTs, including their isomers with a methylation on the 5/5′ and/or 6/6′ position, was achieved with two silica Waters Acquity UHPLC HEB Hilic (150 mm × 2.1 mm; 1.7 μm) columns, preceded by a guard column of the same material. GDGTs were eluted isocratically with 82% *n*-hexane and 18% *n*-hexane:isopropanol (9:1, *v*/v) for 25 min and then with a linear gradient to 30% *n*-hexane:isopropanol (9:1, v/v) for 25 min with a flow rate of 0.2 mL/min. The different GDGTs were detected using selected ion monitoring of the $[M + H]^+$-ions. Quantification was achieved by calculating the area of their corresponding peaks in the chromatogram compared to that of the internal standard.

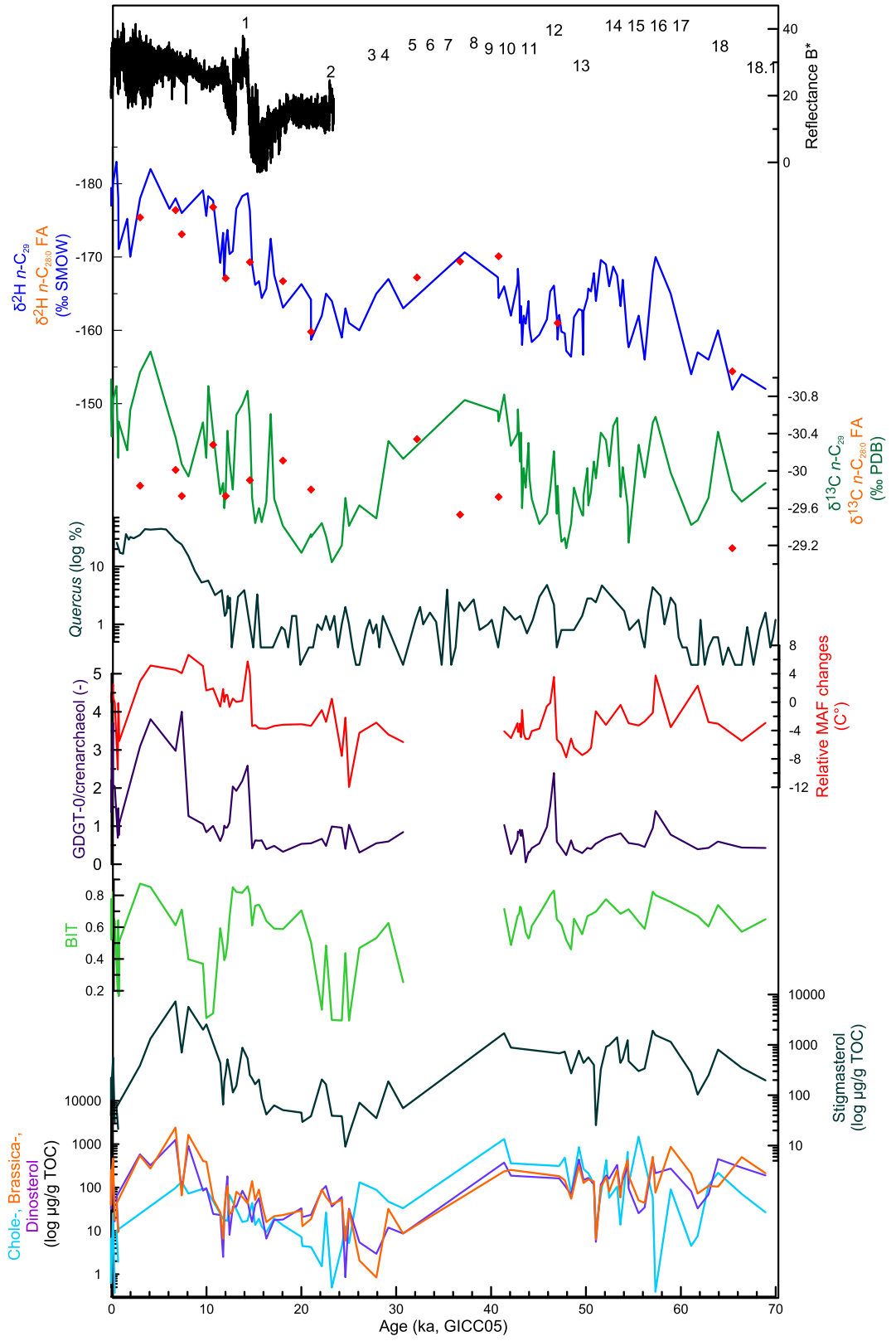

Fig. 2. Proxies from Lake Van, Turkey over 70 kyr: lake-level dynamics (Lake Van B* reflectance; Stockhecke et al., 2016) with numbers for each interstadial; hydrogen and carbon isotopes from leaf waxes and fatty acids, deciduous *Quercus* pollen percentage from Lake Van (on logarithmic ordinate; Litt et al.; 2014b), the GDGT-0/crenarchaeol ratio, relative changes in mean air temperature for months above freezing (MAF) based on brGDGTs, Branched and Isoprenoid Tetraether index (BIT index; Hopmans et al., 2004), isomerization ratio (IR; De Jonge et al., 2014) and sterols on logarithmic ordinate.

The Branched versus Isoprenoid Tetraether (BIT) index was calculated according to Hopmans et al. (2004), and adjusted to include both 5- and 6-methyl brGDGTs:

$$BIT = (Ia + IIa + IIa' + IIIa + IIIa')/(Ia + IIa + IIa' + IIIa + IIIa' + crenarchaeol) \quad (1)$$

The temperature sensitivity of brGDGTs is quantified in the degree of methylation of the 5-methyl brGDGTs (De Jonge et al., 2014):

$$MBT'_{5me} = (Ia + Ib + Ic)/(Ia + Ib + Ic + IIa + IIb + IIc + IIIa) \quad (2)$$

Where Roman numerals refer to the molecular structures of the brGDGTs as given in De Jonge et al. (2014). MBT'_{5me} index values were transferred to MAT using the East African lake calibration (Russell et al., 2018):

$$MAT = -1.21 + 32.42 \times MBT'_{5me} \quad (3)$$

3.4. Stable isotopic composition (δ^2H, $\delta^{13}C$) of leaf-wax n-alkanes and fatty acids

The $\delta^{13}C$ and δ^2H of *n*-alkanes and fatty acids were measured in duplicate, using a Trace GC-Ultra gas chromatograph attached to a Thermo Fischer Delta-V isotope ratio mass spectrometer (irMS) via a combustion and high temperature reduction interface, respectively (GC Isolink, Thermo Fischer). The GC coupled to the irMS was equipped with a 30 m DB-5MS fused silica capillary column (i.d. 0.25 mm; 0.25 μm film thickness). The oven temperature was programmed from 70 °C to 300 °C at a rate of 4 °C/min, followed by an isothermal period of 15 min. Helium was used as a carrier gas. The sample was injected in splitless mode at 275 °C. Raw isotope values were initially converted to the international standard VPDB and VSMOW scale using Thermo Isodat 3.0 software and pulses of a monitoring gas that was measured at the beginning and end of each analysis. Sample $\delta^{13}C$ and δ^2H values were further corrected using the slope and intercept of measured and known values of the C3 *n*-alkane standard mix from Arndt Schimmelmann (Indiana University; *n*-C_{17}: $\delta^{13}C = -31.16‰$, $\delta^2H = -142.4‰$; *n*-C_{19}: $\delta^{13}C = -33.17‰$, $\delta^2H = -118.0‰$; *n*-C_{21}: $\delta^{13}C = -29.10‰$, $\delta^2H = -214.7‰$; *n*-C_{23}: $\delta^{13}C = -31.77‰$, $\delta^2H = -48.8‰$; *n*-C_{25}: $\delta^{13}C = -28.48‰$, $\delta^2H = -254.1‰$) which were run at the beginning and end of each sequence, as well as after every 8 to 10 sample injections. Analytical reproducibility was in the range of 0.2‰ for $\delta^{13}C$ and 2–3‰ for δ^2H.

4. Results and discussion

4.1. Bulk geochemical properties and climate change

Previous studies have indicated that climatic changes during the last six glacial/interglacial cycles and during stadial/interstadial transitions are reflected in the sediment cores by the B* reflectance and TOC (Stockhecke et al., 2014b, 2016). We used the data to relate the results of this study to existing chronostratigraphic data. In Fig. 2, the B* reflectance trends clearly depict rising temperatures from Last Glacial Maximum (LGM) to the Bølling-Allerød (BA) and from Younger Dryas (YD) to the Holocene, as indicated by *Quercus* pollen abundances (Litt et al., 2014). During the Holocene, the TOC values increase up to its maximum around 2 kyr BP (Supplementary Materials - Table 1). Dansgaard-Oeschger interstadials also correspond with increased B* reflectance reflecting rising humidity and more favorable climatic conditions for fauna and flora (Fig. 2).

4.2. Paleotemperature reconstruction

4.2.1. Sources and temperature sensitivity of brGDGTs in Lake Van sediments

BrGDGTs were detected throughout the core, and were dominated by pentamethylated compounds, comprising on average 42% (range 22–69%) of the total brGDGT pool in the sediments, followed by hexamethylated (average 32%, range 16–59%) and tetramethylated brGDGTs (average 25%, range 6–52%). Downcore variations in brGDGT distributions are quantified in the MBT'_{5me} index (Eq. (2)), which varies between 0.21 and 0.79 in the Lake Van record. The MBT'_{5me} index captures the empirically determined brGDGT response to temperature in a set of globally distributed soils (Weijers et al., 2007; De Jonge et al., 2014). However, application of this relationship to lake records has revealed a 'cold bias' in obtained temperatures, which has been coupled to the existence of an additional, in situ source of brGDGTs in lakes that is characterized by higher relative abundances of hexa- and pentamethylated brGDGTs compared to in catchment soils (Tierney and Russel, 2009; Sinninghe Damsté et al., 2009; Tierney et al., 2010; Dang et al., 2018). Subsequent studies have provided evidence for the production of brGDGTs in lakes based on the distinct carbon isotopic compositions of brGDGTs in lakes and those in surrounding soils (Colcord et al., 2017; Weber et al., 2015, 2018) and the identification of a brGDGT isomer that is so far exclusively detected in lakes (Weber et al., 2015). Water column studies indicate that brGDGTs are mainly produced below the oxycline (Sinninghe Damsté et al., 2009; Buckles et al., 2014; Miller et al., 2018; Weber et al., 2018; van Bree et al., 2020), and that temporal variations in production may introduce a temperature bias to the season with the highest brGDGT production (Buckles et al., 2014; Loomis et al., 2014). Sediment trap data from Lake Van indicate that brGDGT fluxes in settling particles collected monthly over one seasonal cycle 10 m above the lake bottom are highest during spring (Huguet et al., 2012), suggesting either increased soil input or lacustrine production at this time. Since the brGDGT composition in soils around Lake Van is not known and a comparison with brGDGTs in the lake sediments is not possible, we here follow the findings of previous studies and assume that brGDGTs in Lake Van are mainly produced in situ. A global lake-specific calibration that considers the full suite of brGDGT isomers is not (yet) available, but the calibration based on East African lakes uses the MBT'_{5me} index to estimate temperatures (Russell et al., 2018). The relation between temperature and the degree of methylation of aquatic brGDGTs has recently been confirmed in a microcosm experiment (Martínez-Sosa et al., 2020), providing confidence in the use of the MBT'_{5me} index to derive a temperature record. To accommodate uncertainties in the sources of brGDGTs through time and the ability of the East African lake calibration to obtain reliable temperature estimates for Lake Van, we base our discussion on a normalized temperature record obtained after application of the MBT'_{5me} index and the East African lake calibration and only focus on the timing, direction and relative amplitude of temperature changes inferred from the brGDGT signals.

4.2.2. Temperature variability in eastern Anatolia

The normalized brGDGT-based temperature record indicates strong fluctuations in temperature over the past 70 kyr, within a range of ~17 °C (Figs. 2, 3a, b). The brGDGTs indicate that air temperature increased with ~9 °C over the last deglaciation (Fig. 3a), tracking the sudden onset of the BA in B* reflectance. This warming trend is interrupted by the YD, after which temperatures increase again to values higher than present-day MAT, reaching a maximum between 6 and 3 kyr (Fig. 3a). The amplitude of deglacial warming at Lake Van is higher than the rise of 6–7 °C in SST reported for the eastern Mediterranean based on marine U^K_{37}' data (Emeis et al., 2003), which may be attributed to a possible bias towards summer temperatures in the brGDGT record resulting from seasonal variations in brGDGT production/flux towards the sediment (Huguet et al., 2012). The high seasonality at Lake Van (temperature fluctuates between −13 and 20 °C in the modern system) suggests that the brGDGT record likely represents a temperature signal for months above freezing (MAF) rather than MAT, as has also been established for soils (Naafs et al., 2017; Dearing Crampton-Flood et al., 2020).

During MIS3, brGDGTs have recorded the millennial scale temperature variations that characterize this period (Fig. 3). In general,

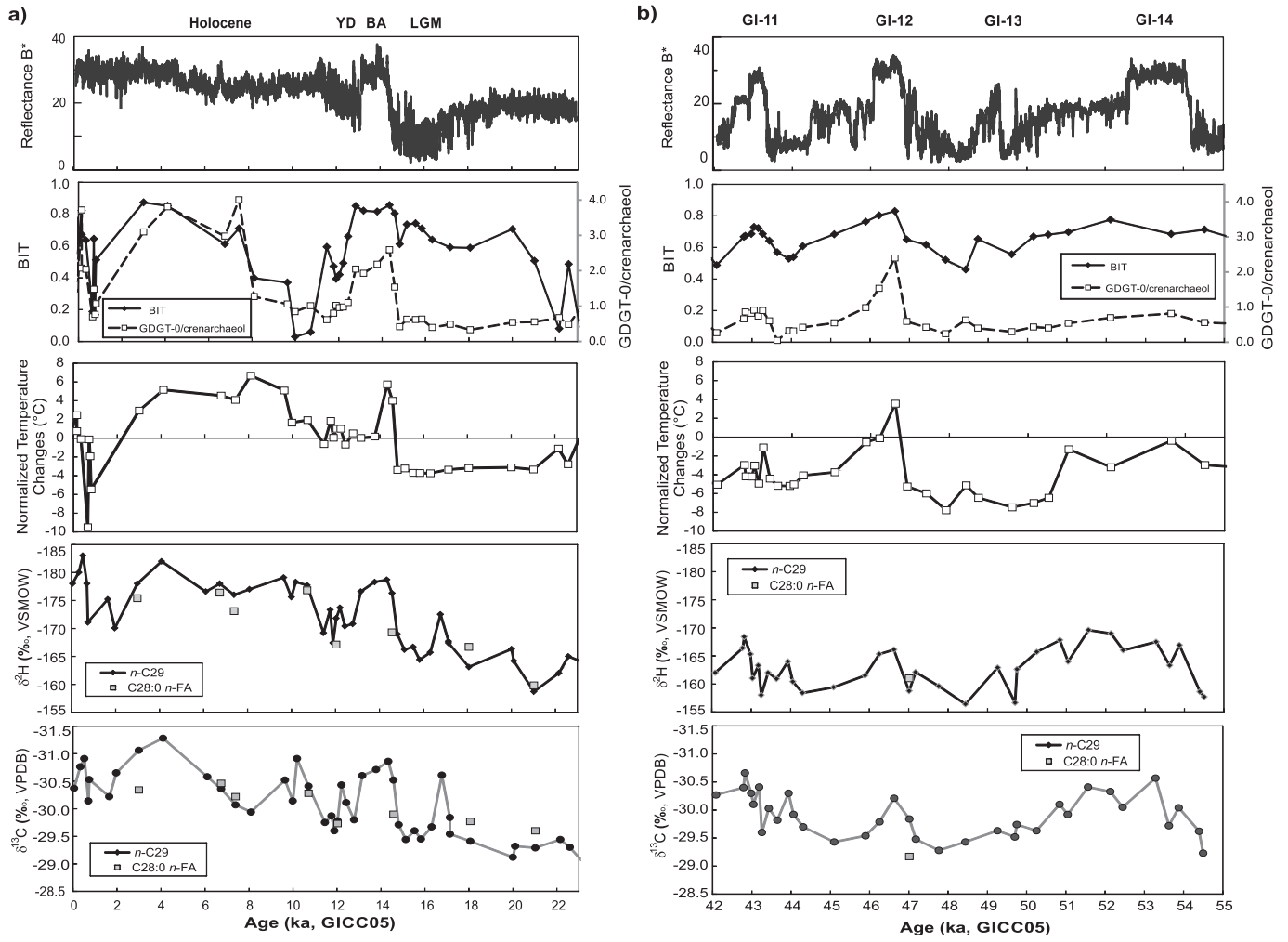

Fig. 3. Color index (Reflectance B*) as climatic proxy, the Branched and Isoprenoid Tetraethers (BIT) index and GDGT-0/crenarchaeol ratios, relative changes in mean air temperatures for months above freezing (MAF), and the hydrogen and carbon isotopic compositions of C_{29} *n*-alkane and the $C_{28:0}$ *n*-fatty acid (FA) during (a) the Last Glacial Maximum (LGM) to present, and (b) several Dansgaard-Oeschger events (11 to 14).

temperatures are higher during interstadials 11 to 14 and lower during stadials, in line with the interpretation of other proxy records, such as pollen (Pickarski et al., 2015) and TOC determined for the same sediment core (Figs. 3b, 5b). The amplitude of the temperature fluctuations during the stadials and interstadials is of the same order as the glacial/interglacial temperature difference. However, the relative changes in temperature of up to 8 °C during DO events (Figs. 2, 3b) are larger than those reflected by TEX_{86}-based SSTs for the Black Sea (Wegwerth et al., 2015) and alkenone-based SSTs from the western Mediterranean (Martrat et al., 2004) that indicate changes of ~4–6 °C. Beside the summer bias of the brGDGTs, the amplitude of temperature changes at Lake Van may well be enhanced due to its more inland location making it more sensitive to climate variability.

4.3. Hydroclimate reconstruction

4.3.1. Hydrogen isotopes of plant leaf waxes

In the sediment profile, δ^2H values of long-chain *n*-alkanes (i.e. *n*-C_{29}) derived from leaf wax lipids of terrestrial plants vary from −183 to −159‰ with generally higher values during the last glaciation and the YD in comparison with the BA and the Holocene (Figs. 2, 3a). The hydrogen isotopic compositions of the *n*-C_{28} saturated long-chain fatty acids, measured in selected samples, depict a similar trend in δ^2H as the *n*-C_{29} alkane. As seen in the temperature records, high-frequency variations between −183 and − 170‰ are obtained during late Holocene (0–4 kyr BP). The results are in agreement with early Holocene hydroclimatic variability in the Lake Neor region NW Iran (Aubert et al., 2017) inferred from chironomids and pollen analyses showing the same trends at lower resolution. During Dansgaard-Oeschger events, the δ^2H values show minor variations between −170 and - 156‰ (Figs. 2, 3b). Relatively high δ^2H values of *n*-C_{29} between −152 and − 168‰ are observed frequently during glacial and stadial periods (Figs. 2, 3a, b) characterized by cooler and dryer climate (Litt et al., 2014).

In the Lake Van region, strong seasonal temperature variations occur today (−13 and 20 °C) and δ^2H_{precip} values change accordingly between −120 and 0‰ VSMOW (IAEA/WMO, 2014). If we use only the time window for plant growth (April to July), the δ^2H signal of precipitation and hence water used for growth is between −30 and − 50‰VSMOW today. These periods of increased seasonal production are supported by highest input of pollen and leaf wax *n*-alkanes into the sediments based on sediment trap data (Huguet et al., 2012). Plant source-water δ^2H values are reported to generally follow those of precipitation (West et al., 2007). If we assume a stable isotope fractionation of 120 to 130‰ between δD precipitation and δ^2H of *n*-C_{29} (Sachse et al., 2012), δ^2H values of precipitation of around −50‰ are reconstructed based on the δ^2H_{C29} in the surface sediments (−180‰). This value is in general agreement with measured δ^2H_{precip} in the Lake Van region during the growth season. As the samples investigated include sediments

accumulated over a decade or less, δ^2H of plant lipids provide information about the average isotopic composition of precipitation during biosynthesis over these periods. Differences in δ^2H of precipitation within the time intervals investigated could be caused by persistent changes in air temperature or humidity (p/e ratio).

A temperature control on δ^2H of leaf-wax *n*-alkanes during MIS3 to MIS1 can be considered minor, because warmer climatic conditions should result in higher δ^2H. Based on the narrow range in $\delta^{13}C$ of leaf-wax lipids, the influence of changes in vegetation composition (i.e. C_3 versus C_4 plants) and/or type on δ^2H values can also be considered minor. The pollen assemblages indicate *Artemesia* steppe vegetation during glacials and the predominance of oak and pine trees during interglacials (Litt et al., 2014; Pickarski et al., 2015). The positive relationship between $\delta^{13}C$ and δ^2H values measured on long-chain *n*-alkanes (Figs. 2, 3) can be interpreted in terms of stomatal constraint on leaf gas-exchange mediated by water supply (Randlett et al., 2017). Hence, we conclude that the δ^2H values can be interpreted as changes in p/e ratio. Based on intervals measured at high resolution (Termination 1; DO events during MIS3), *n*-C_{29} alkanes show more depleted δ^2H values during warmer periods, whereas higher δ^2H values are obtained for cooler intervals (Figs. 3a, b).

The record indicates warmer and more humid conditions during interglacials and interstadials and cooler and arid conditions during glacials and stadials. The δ^2H values of saturated long-chain fatty acids are in line with the variations obtained from *n*-alkanes (δ^2H of *n*-$C_{26:0}$ and *n*-$C_{28:0}$ FAs vary between −154 and − 174‰). Based on the difference between the δ^2H values of algal-derived *n*-$C_{18:0}$ and higher plant-derived *n*-$C_{28:0}$ FAs, the extent of evapotranspiration may be estimated. A comparable approach has been introduced by Sachse et al. (2006) using the short-chain (*n*-C_{17}, *n*-C_{19}, *n*-C_{21}) and the long-chain (*n*-C_{27}, *n*-C_{29}, *n*-C_{31}) alkanes as proxies for aquatic organisms versus terrestrial flora. In contrast to leaf water used for lipid biosynthesis in land plants, δ^2H of source water available to aquatic OM production is not affected by evapotranspiration. This leads to increased differences in δ^2H of long- and short-chain *n*-alkanes during dry conditions. As the concentration of short-chain *n*-alkanes was too low for H-isotope analyses, short- and long-chain saturated fatty acids were measured instead. Based on a limited number of analyses, the largest offsets in δ^2H values (15 to 20‰) are obtained for cold and dry intervals, whereas smaller differences in δ^2H values (9 to 15‰) are observed for periods during which warm and humid conditions prevailed (Fig. 4). The results indicate increased evapotranspiration and aridity during cooler intervals and higher humidity during warm periods. The low δ^2H values of *n*-C_{29}, obtained within the 6–3 kyr BP interval, are consistent with the maximum in brGDGT-based normalized temperature changes (Fig. 3a) and the proposed climate optimum during the Holocene due to increased humidity between 6.2 and 4 kyr BP (Wick et al., 2003).

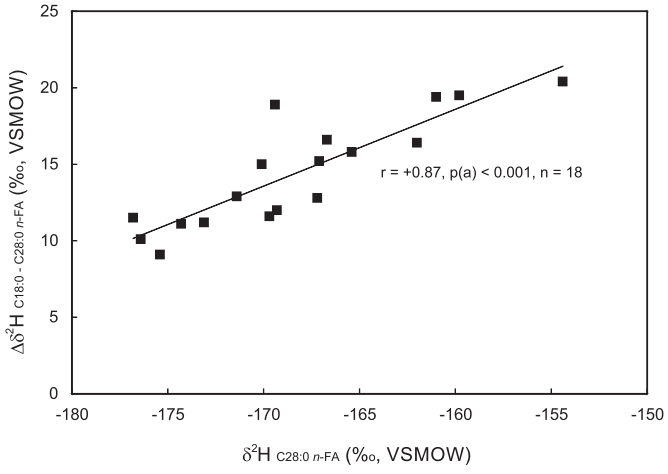

Fig. 4. Correlation diagram of δ^2H of $C_{28:0}$ *n*-FA versus the difference in δ^2H of $C_{18:0}$ and $C_{28:0}$ *n*-FAs.

4.3.2. Estimates of precipitation changes

Isotopically 10‰ lighter δ^2H-values of leaf-wax *n*-alkane C_{29} argue for a substantially increased humidity during the interstadials compared to the stadials. During the interglacials compared to the glacials 20‰ lighter δ^2H-values indicate an even larger increased humidity (Figs. 2, 3).

Estimates of the magnitude of precipitation changes can be made based on variation in δ^2H of leaf wax *n*-alkanes from specific plant species in relation to meteorological data for the growth area. Unfortunately, such data are so far only available from C_3 and C_4 grass *n*-alkane isotopic ratios from the Great Plains (USA). The data indicate a ~ 10‰ increase in the apparent enrichment factor between C_{29} *n*-alkanes and the δ^2H value of precipitation per 200 mm increase in annual precipitation, including the overall effect of evapotranspiration (Smith and Freeman, 2006). The application of this relationship results in precipitation increases of about 200 mm per year during DO interstadials and of 300–350 mm per year during interglacials.

4.3.3. Water column conditions

Initially, the branched and isoprenoid tetraether (BIT) index was proposed to determine the relative input of soil organic matter into an aquatic system, where brGDGTs represent soil material, and crenarchaeol, an isoprenoid GDGT produced by Thaumarchaeota in aquatic environments, represents the aquatic endmember (Hopmans et al., 2004). In Lake Van, BIT index values vary between 0 and 1, which would imply that the contribution of soil organic matter, and thus brGDGTs, to the lake sediments have substantially varied through time (Figs. 2, 3a,b). However, changes in the BIT index may also be the result of fluctuations in crenarchaeol production, which mostly takes place in the upper water layer above the oxycline (Buckles et al., 2013, 2014). Indeed, the BIT index for settling particles collected 10 m above the lake floor of Lake Van appeared to be insensitive to changes in brGDGT concentration and were instead driven by the flux of crenarchaeol (Huguet et al., 2012). The BIT index shows a significant negative correlation ($r = -0.54$, p(a) < 0.005, $n = 86$) with crenarchaeol concentrations in the sediment core, indicating that crenarchaeol production is also the main driver of the BIT index over longer timescales (Fig. 5a, Supplementary Materials - Table 1). Hypothetically, the production of crenarchaeol could be reduced during periods with a shallow oxycline, which narrows the niche of their producers in the water column (Kumar et al., 2019). This implies that variations in the BIT index may be linked to (climate-driven) changes in lake mixing regime. Indeed, the BIT index record mostly follows the color record reflecting the total organic matter (TOC) in the sediment (Fig. 3; Stockhecke et al., 2014b), where high BIT values coincide with the high TOC concentrations that would result from enhanced production and subsequent preservation under a stratified water column during warm and wet conditions (Fig. 3). The occurrence of water column stratification and thus expansion of the anoxic zone deeper in the lake during warmer and wetter climate conditions is supported by the simultaneous increases in the isoGDGT-0/crenarchaeol ratio during interstadials and the Holocene (Fig. 3, 5b), which indicates an enhanced contribution of methanogenic archaea to the pool of isoprenoid GDGTs stored in the lake sediment (Blaga et al., 2009).

4.4. Vegetation and aquatic community reconstruction

4.4.1. Changes in vegetation cover and type

The alkane distribution in all samples is dominated by long chain *n*-alkanes with a marked odd over even carbon number predominance typical for land plants (Bray and Evans, 1961; Eglinton and Hamilton, 1967). The *n*-C_{29} is the most abundant alkane, except in the sediments deposited during the earliest Holocene (after Termination 1), when *n*-C_{31} and *n*-C_{29} alkanes are present in similar amounts. The variation in

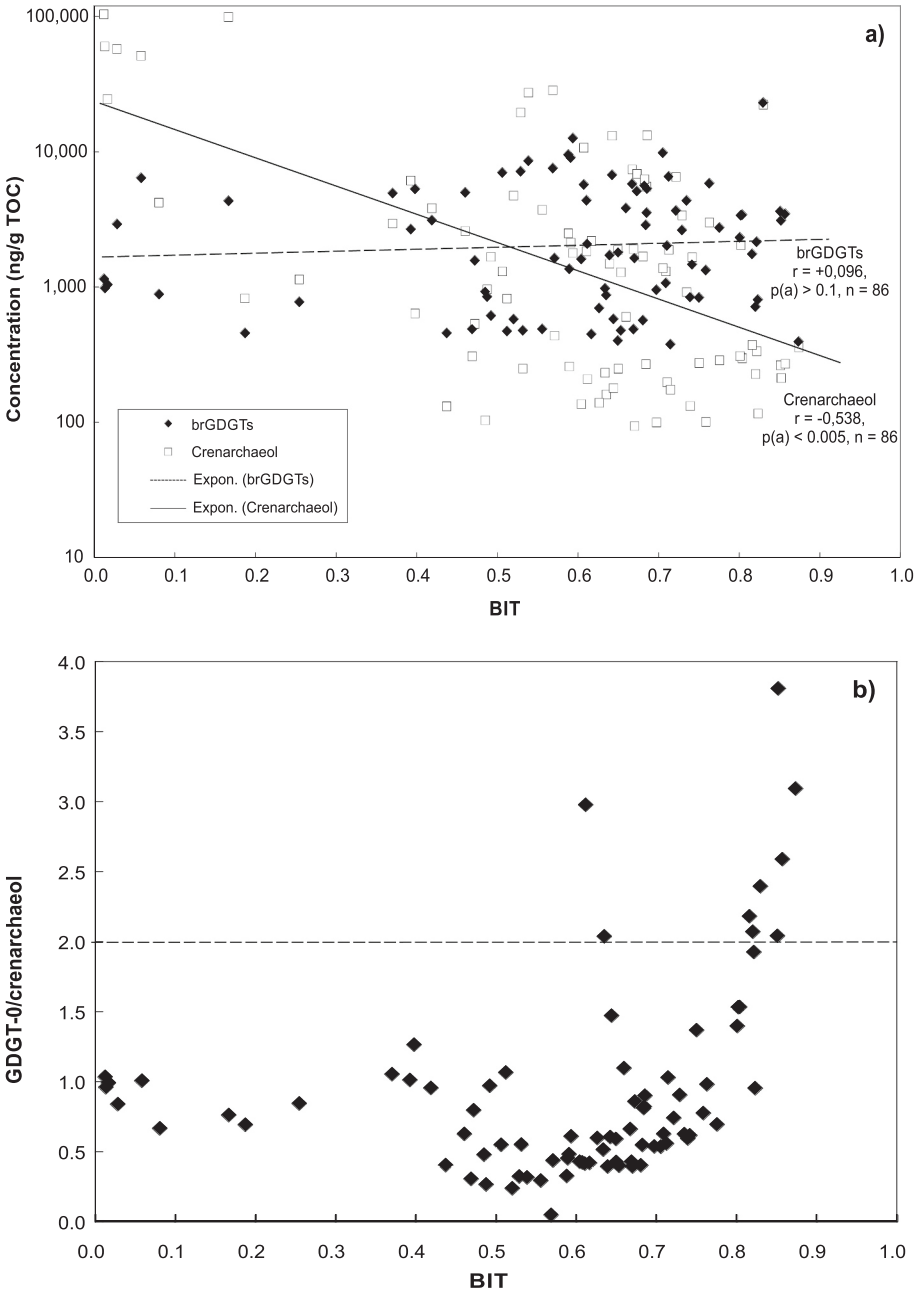

Fig. 5. Cross-correlations of (a) crenarchaeol and brGDGTs concentrations versus BIT, and (b) isoGDGT-0/crenarchaeol ratios versus BIT index values.

TOC-normalized plant waxes (C_{27}, C_{29}, C_{31} *n*-alkanes) during DO events and the last glacial termination is shown in Fig. 6. Interstadials (GI-13, GI-14, BA) are characterized by increased abundances of plant wax *n*-alkanes, reflecting the expansion of higher land plants during warmer and wetter periods (Fig. 6b). However, high abundances of *n*-alkanes do not always (e.g. prior to GI-14, and during LGM) correspond to intervals of favorable climatic conditions for the expansion of higher land plants (Figs. 6a, b). This could be explained by increased soil input, containing organic matter of predominantly terrigenous origin, after drier stadials due to intensified precipitation.

Over the whole period, the $\delta^{13}C$ values of *n*-C_{29} alkane in Lake Van sediments vary within a narrow range from −29.4 to −31.3‰ (Figs. 3a, b). The values fall between the ranges typical of *n*-alkanes of C_3 plants (around - 35‰,) and *n*-alkanes of C_4 plants (around −25‰; Chikaraishi and Naraoka, 2003). The marginal change in $\delta^{13}C$ of long-chain *n*-alkanes could be explained by a minor change of less than 12% in relative contribution of C_4 plants within Lake Van samples (cf. Randlett et al., 2017). This is supported by the pollen record, which indicates that Lake Van was surrounded by a dominantly steppe type vegetation, such as *Artemesia*, *Chenopodiaceae* and *Poaceae* from MIS4 to 2, whereas the Holocene is characterized by a significant contribution of *Quercus* trees (Litt et al., 2014). In the limited number of Lake Van samples, investigated for isotopic composition of fatty acids, the $\delta^{13}C$ values of saturated long-chain *n*-FAs varied only marginally i.e. between −28.2 and −30.3‰ (Figs. 3a, b). The results are consistent with the data from leaf-wax *n*-alkanes, indicating a minor shift in vegetation within the Lake Van profile. These small floral changes can only account for a negligible effect on the variability of $\delta^{2}H$ of *n*-C_{29} alkane observed in the core.

The covariation of $\delta^{13}C$ with $\delta^{2}H$ indicates an influence of moisture stress on ^{13}C concentrations in the plants (i.e. more enriched $\delta^{13}C$ values during dry conditions). Beside of the effect of stomatal aperture on isotopic composition of *n*-alkanes, the trend in $\delta^{13}C$ of *n*-C_{29} towards

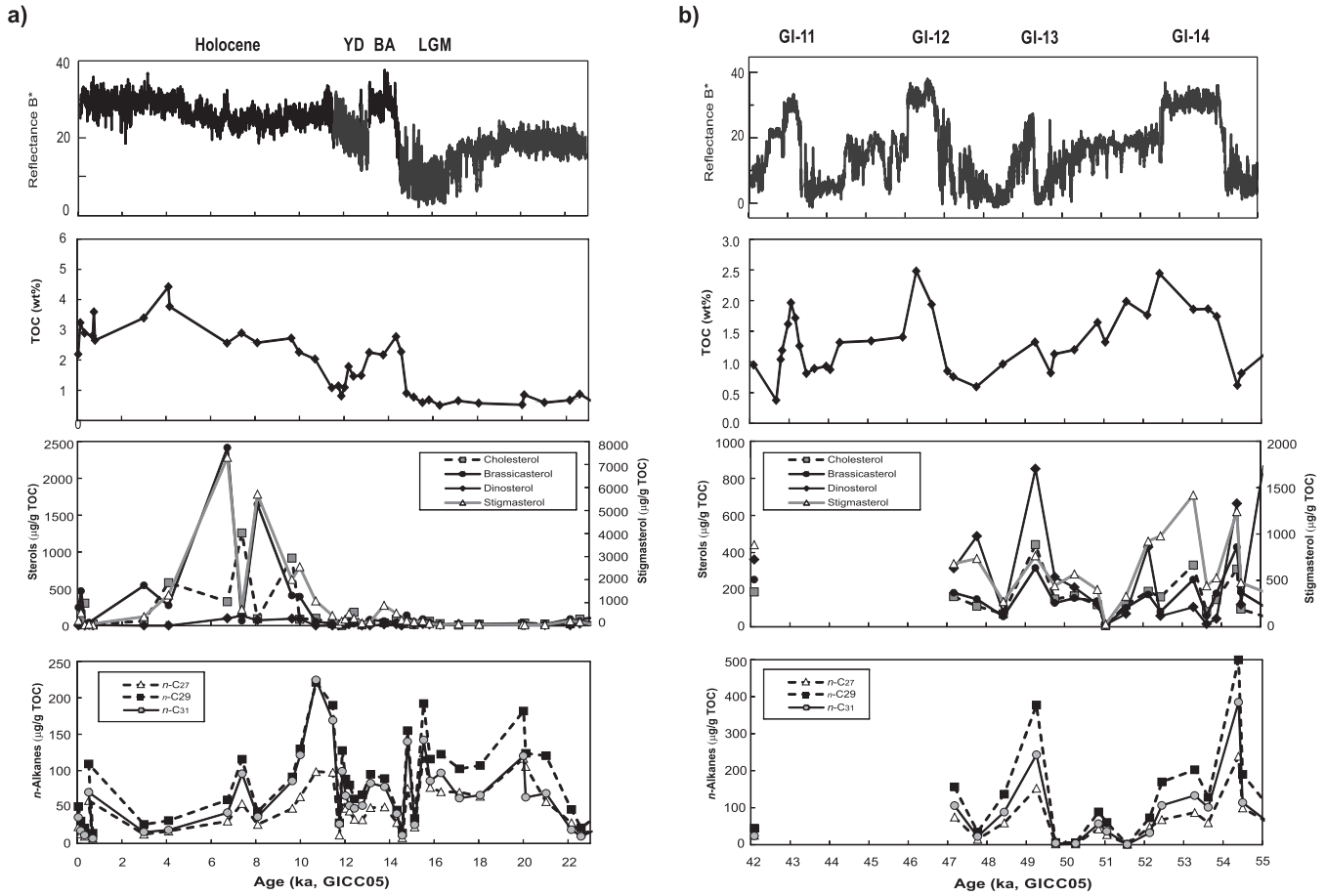

Fig. 6. Color index (Reflectance B*), total organic carbon contents (TOC), and TOC-normalized concentrations of sterols and long-chain *n*-alkanes, respectively, during (a) the Last Glacial Maximum (LGM) to present, and (b) several Dansgaard-Oeschger events (11 to 14).

lighter values from 22 kyr to present (Fig. 3a) may indicate a minor change from C_4 to more C_3 plants.

4.4.2. *Aquatic community variability*

Sterols are present in considerable concentrations throughout both intervals (44–11,072 µg/g TOC), and are mostly dominated by stigmasterol (24-ethylcholesta-5,22-dien-3β-ol), cholesterol (cholest-5-en-3β-ol), and brassicasterol (24-methylcholesta-5.22-dien-3β-ol). Stigmasterol has been reported to be a typical marker of higher plant input and marsh grasses (Canuel et al., 1997). However, there is also evidence for microalgal and cyanobacterial sources of these compounds (Volkman et al., 1999; Rontani and Volkman, 2005). Highest concentrations of stigmasterol are observed during interglacial and interstadial periods. Stigmasterol is the most abundant sterol (Figs. 2 and 6a, b), especially during the Holocene and GI-14. The trends reflect the increase in lake level due to freshwater inflow promoting algal blooms in the lake and increased vegetation density during periods of warmer climate and increased humidity (Litt et al., 2014; Stockhecke et al., 2016; Randlett et al., 2017).

Brassicasterol is considered as a diatom marker (Brassell et al., 1982; Killops and Killops, 1997). Within the periods selected for high-resolution analyses, brassicasterol shows increased concentrations during DO interstadials (Fig. 6b) and especially in several intervals during the Holocene (e.g. 6.7, 8.1 BP; Fig. 6a). These intervals most probably reflect periods of increased freshwater inflow, neutralization of the alkaline water body and a better diatom preservation (Stockhecke et al., 2014b).

Cholesterol has been used to indicate inputs from zooplankton grazing in the water column (Gagosian et al., 1983), although it has also been reported as an algal/phytoplankton marker (Volkman et al., 1998). The positive correlation between cholesterol and stigmasterol as well as brassicasterol concentrations implies increasing bioproductivity and flourishing zooplankton communities during interstadials and interglacials.

Dinosterol (4-methyl-23,24-dimethylcholest-22-en-3b-ol), a marker for dinoflagellates (Volkman, 2003), occurs in low concentrations in Lake Van sediments. Despite an increase during MIS3, the overall low concentrations of dinosterol indicate a minor contribution of dinoflagellates to total biomass production, restricted to intervals characterized by warmer and humid climate (Figs. 6a, b).

The general increase in biomass production during warmer and wetter periods may have contributed to the shallowing of the oxycline reflected by the BIT index (Fig. 3), and the subsequent expansion of anaerobic conditions indicated by the GDGT-0/crenarchaeol ratio (Fig. 3).

4.5. *Comparison with terrestrial and marine paleoclimate reconstructions*

Comparison of our multi-proxy records from Lake Van with continental Eastern Mediterranean paleoclimate reconstructions based on Sofular cave speleothem oxygen isotopes (Badertscher et al., 2011) and pollen assemblages from Lago Grande di Monticchio (Allen et al., 1999) reveals a consistent picture (Fig. 7), and implies that the climate dynamics recorded in Lake Van are valid for the larger Eastern Mediterranean (Fig. 7). As the Sofular $\delta^{18}O$, an indicator of Black Sea hydrology inferred from surface water changes related to the presence or absence of a connection to the Mediterranean Sea, and the Monticchio woody taxa record are both qualitative indicators of precipitation changes, no

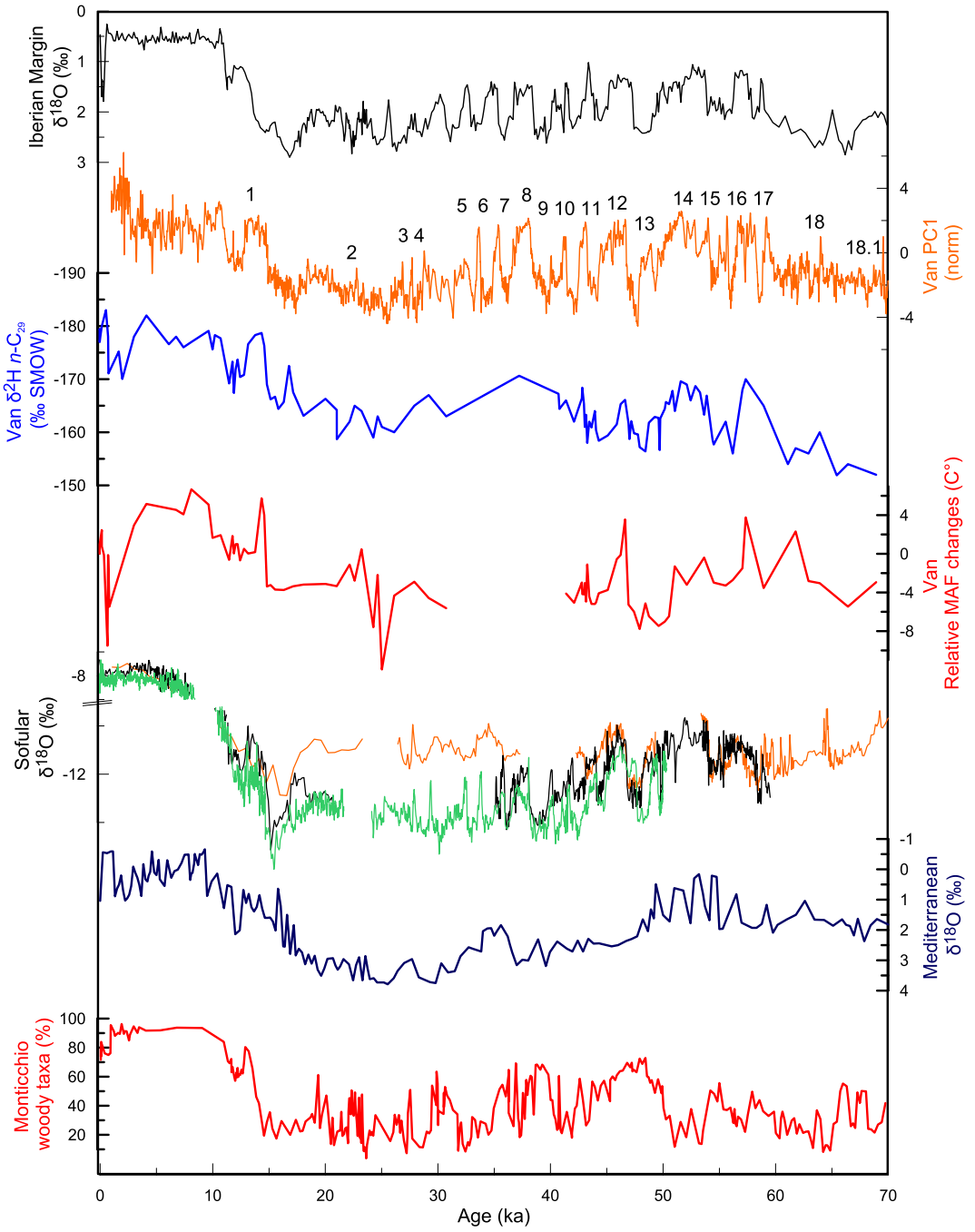

Fig. 7. Comparison of different paleo-archives over 70 kyr from the North Atlantic, Turkey and the Mediterranean: $\delta^{18}O$ of planktic foraminifera from Iberian Margin (Hodell et al., 2013); Hydroclimate PC1 for Lake Van (Stockhecke et al., 2016) with numbers for each interstadial; isotopic composition of leaf wax C_{29} *n*-alkane and the $C_{28:0}$ *n*-FA (this study), relative changes in mean air temperatures for months above freezing (MAF, this study), $\delta^{18}O$ from the Sofular cave (Badertscher et al., 2011); $\delta^{18}O$ from the Eastern Mediterranean Sea (Kroon et al., 1998; Almogi-Labin et al., 2009), and woody taxa from the Lago Grande di Monticchio (Allen et al., 1999). All data are shown on their original timescales.

absolute comparisons can be made. Regardless, in particular the last termination including the BA-YD succession and the variability of DO events 12, 13 and 14 are similarly recorded at all three sites (Fig. 7). All these records point towards warmer and wetter climate conditions during interstadials and interglacials, which is supported by LOVECLIM simulation model outcomes (Hydroclimate PC1, Stockhecke et al., 2016). This model revealed that droughts in the Eastern Mediterranean during glacials/stadials are a large-scale phenomenon, associated with stronger mean annual anticyclonic circulation and increased atmospheric subsidence (not shown here) in the Eastern Mediterranean and typically cold surface conditions in the North Atlantic. The relationship between our proxy records and the model outputs suggests that an increase of precipitation at Lake Van is a consequence of enhanced moisture transport towards the Eastern Mediterranean connected to the strengthening of the Atlantic Meridional Overturning Circulation (AMOC) in the North Atlantic and associated changes in the atmospheric circulation.

Although the trends in carbonate oxygen isotope records from the Iberian Margin (Hodell et al., 2013) and Eastern Mediterranean Sea (Kroon et al., 1998; Almogi-Labin et al., 2009) present the same overall

picture, the marine records reflect slightly more stable conditions as opposed to the pronounced millennial-scale variability that can be recognized in the records of Black Sea hydrology and vegetation changes in Italy (Fig. 7). Our multi-proxy climate records for Lake Van are in line with previous paleoclimate reconstructions for the Eastern Mediterranean as well as results from a LOVECLIM model simulation and furthermore confirm the occurrence of abrupt (hydro)climatic changes on land during the past 70 ka.

5. Conclusions

Estimates of temperature and precipitation changes during the last glacial-interglacial transitions in the Eastern Mediterranean have so far primarily been based on paleobotanical data or sea surface temperatures. In this study millennial-scale climate variability during MIS3 and the last deglaciation is reconstructed using brGDGTs in combination with hydrogen isotope data obtained from long-chain *n*-alkanes over the last 70 kyr.

BrGDGTs indicate that MAF fluctuates during stadial/interstadial transitions associated with DO events (GI-11 to GI-14). The amplitude of these fluctuates is only slightly exceeded by the degree of atmospheric warming during the last termination. However, to obtain quantitative information on mean annual air temperature changes, a suitable transfer function of brGDGTs from lake sediments of comparable climatic and altitudinal settings is required. The δ^2H of fatty acids and plant wax alkanes reveal that warm periods are characterized by more humid conditions, whereas evapotranspiration and aridity increase during cooler intervals. The linear correlation between $\delta^{13}C$ and δ^2H values measured in long-chain *n*-alkanes C_{29} and C_{31} most probably results from stomatal constraints on leaf gas-exchange mediated by water supply. The apparent enrichment factor between C_{29} *n*-alkanes and δ^2H of precipitation in the modern system translates into an increase in mean annual precipitation of about 200 mm for transitions from stadial to interstadials, and about 300–350 mm for the transitions from glacial to interglacials.

Increased concentrations of sterols in sediment record indicate that algal blooms occurred in Lake Van during periods of warmer climate and increased humidity. These blooms presumably contributed to a shoaling of the chemocline, resulting in niche differentiation and competition for Thaumarchaeota in the oxic water layer reflected by higher BIT index values.

Our multi-proxy climate records are in line with previous paleoclimate reconstructions for the Eastern Mediterranean as well as results from a LOVECLIM model simulation. Together, they confirm the presence of abrupt hydroclimatic changes during the past 70 kyr and support that lake-level increases during warm interstadials are caused by increased precipitation coupled to atmospheric changes as a consequence of strengthening of the Atlantic Meridional Overturning Circulation (AMOC).

Supplementary data to this article can be found online at https://doi.org/10.1016/j.palaeo.2021.110535.

Declaration of Competing Interest

The authors declare that they have no known competing financial interests or personal relationships that could have appeared to influence the work reported in this paper.

Acknowledgements

We thank two anonymous reviewers for constructive comments that helped to improve the manuscript. We also thank the PALEOVAN team for support during collection and sharing of data. The authors acknowledge funding of the Swiss National Science Foundation (SNF) 200021_124981, 200020_143330, P300P2-158501 200020_143340, 20FI21_124972, 200021_124981, and 200020L_156110/1 the PALEOVAN drilling campaign by the International Continental Scientific Drilling Program (ICDP), the Deutsche Forschungsgemeinschaft (DFG) LI 582/20-1, the Scientific and Technological Research Council of Turkey (Tübitak) and the Austrian Science Foundation (FWF Project No. I 2068-N29). Serge Robert is thanked for the help in the laboratory. FP acknowledges financial support from NWO-Vidi grant #192.074.

References

Allen, J.R.M., Brandt, U., Brauer, A., Hubberten, H.W., Huntley, B., Keller, J., Kraml, M., Mackensen, A., Mingram, J., Negendank, J.F.W., Nowaczyk, N.R., Oberhansli, H., Watts, W.A., Wulf, S., Zolitschka, B., 1999. Rapid environmental changes in southern Europe during the last glacial period. Nature 400 (6746), 740–743.

Almogi-Labin, A., Bar-Matthews, M., Shriki, D., Kolosovsky, E., Paterne, M., Schilman, B., Ayalon, A., Aizenshtat, Z., Matthews, A., 2009. Climatic variability during the last 90 ka of the southern and northern Levantine Basin as evident from marine records and speleothems. Quat. Sci. Rev. 28 (25–26), 2882–2896.

Andersen, K., Azuma, N., Barnola, J., Bigler, M., Biscaye, P., Caillon, N., Chappellaz, J., Clausen, H., Dahl-Jensen, D., Fischer, H., Fluckiger, J., Fritzsche, D., Fujii, Y., Goto-Azuma, K., Gronvold, K., Gundestrup, N., Hansson, M., Huber, C., Hvidberg, C., Johnsen, S., Jonsell, U., Jouzel, J., Kipfstuhl, S., Landais, A., Leuenberger, M., Lorrain, R., Masson-Delmotte, V., Miller, H., Motoyama, H., Narita, H., Popp, T., Rasmussen, S., Raynaud, D., Rothlisberger, R., Ruth, U., Samyn, D., Schwander, J., Shoji, H., Siggard-Andersen, M., Steffensen, J., Stocker, T., Sveinbjornsdottir, A., Svensson, A., Takata, M., Tison, J., Thorsteinsson, T., Watanabe, O., Wilhelms, F., White, J., Project, N.G.I.C, 2004. High-resolution record of Northern Hemisphere climate extending into the last interglacial period. Nature 147–151.

Aubert, C., Brisset, E., Djamali, M., Sharifi, A., Ponel, P., Gambin, B., Azirani, T.A., Guibal, F., Lahijani, H., Beni, A.N., de Beaulieu, J.-L., Pourmand, A., Andrieu-Ponel, V., Thiéry, A., Gandouin, E., 2017. Late glacial and early Holocene hydroclimate variability in Northwest Iran (Talesh Mountains) inferred from chironomid and pollen analysis. J. Paleolimnol. 58, 151–167.

Badertscher, S., Fleitmann, D., Cheng, H., Edwards, R.L., Gokturk, O.M., Zumbuhl, A., Leuenberger, M., Tuysuz, O., 2011. Pleistocene water intrusions from the Mediterranean and Caspian seas into the Black Sea. Nat. Geosci. 4 (4), 236–239.

Blaga, C., Reichart, G.J., Heiri, O., Sinninghe Damsté, J.S., 2009. Tetraether membrane lipid distributions in lake particulate matter and sediments: a study of 47 European lakes along a north–south transect. J. Paleolimnol. 41, 523–540.

Blockley, S.P.E., Lane, C.S., Hardiman, M., Rasmussen, S.O., Seierstad, I.K., Steffensen, J. P., Svensson, A., Lotter, A.F., Turney, C.S.M., Ramsey, C.B., INTIMATE members, 2012. Synchronisation of palaeoenvironmental records over the last 60,000 years, and an extended INTIMATE1 event stratigraphy to 48,000 b2k. Quat. Sci. Rev. 36, 2–10.

Brassell, S.C., Eglinton, G., Maxwell, J.R., 1982. Chemical fossils: the geological fate of steroids. Science 217, 491–504.

Bray, E.E., Evans, E.D., 1961. Distribution of n-paraffins as a clue to recognition of source beds. Geochim. Cosmochim. Acta 22, 2–15.

Buckles, L.K., Villanueva, L., Weijers, J.W.H., Verschuren, D., Sinninghe Damsté, J.S., 2013. Linking isoprenoidal GDGT membrane lipid distributions with gene abundances of ammonia-oxidizing Thaumarchaeota and uncultured crenarchaeotal groups in the water column of a tropical lake (Lake Challa, East Africa). Environ. Microbiol. 15, 2445–2462.

Buckles, L.K., Weijers, J.W.H., Verschuren, D., Sinninghe Damsté, J.S., 2014. Sources of core and intact branched tetraether membrane lipids in the lacustrine environment: anatomy of Lake Challa and its catchment, equatorial East Africa. Geochim. Cosmochim. Acta 140, 106–126.

Canuel, E., Freeman, K., Wakeham, S., 1997. Isotopic compositions of lipid biomarker compounds in estuarine plants and surface sediments. Limnol. Oceanogr. 42, 1570–1583.

Chikaraishi, Y., Naraoka, H., 2003. Compound-specific delta D-delta C-13 analyses of n-alkanes extracted from terrestrial and aquatic plants. Phytochemistry 63, 361–371.

Colcord, D.E., Pearson, A., Brassell, S.C., 2017. Carbon isotopic composition of intact branched GDGT core lipids in Greenland lake sediments and soils. Org. Geochem. 110, 25–32.

Dang, X., Ding, W., Yang, H., Pancost, R.D., Naafs, B.D.A., Xue, J., Lin, X., Lu, J., Xie, S., 2018. Different temperature dependence of the bacterial brGDGT isomers in 35 Chinese lake sediments compared to that in soils. Org. Geochem. 119, 72–79.

De Jonge, C., Hopmans, E.C., Zell, C.I., Kim, J.-H., Schouten, S., Sinninghe Damsté, J.S., 2014. Occurrence and abundance of 6-methyl branched glycerol dialkyl glycerol tetraethers in soils: implications for palaeoclimate reconstruction. Geochim. Cosmochim. Acta 141, 97–112.

Dearing Crampton-Flood, E., Tierney, J.E., Peterse, F., Kirkels, F.M.S.A., Sinninghe Damsté, J.S., 2020. BayMBT: a Bayesian calibration model for branched glycerol dialkyl glycerol tetraethers in soils and peats. Geochim. Cosmochim. Acta 268, 142–159.

Degens, E.T., Kurtman, F., 1978. The Geology of Lake Van. MTA Press, Ankara.

Djamali, M., de Beaulieu, J.-L., Shah-hosseini, M., Andrieu-Ponel, V., Ponel, P., Amini, A., Akhani, H., Leroy, S.A.G., Stevens, L., Lahijani, H., Brewer, S., 2008. A late Pleistocene long pollen record from Lake Urmia, NW Iran. Quat. Res. 69, 413–420.

Eglinton, G., Hamilton, R.J., 1967. Leaf epicuticular waxes. Science 156, 1322–1335.

Emeis, K.C., Schulz, H., Struck, U., Rossignol-Strick, M., Erlenkeuser, H., Howell, M.W., Kroon, D., Mackensen, A., Ishizuka, S., Oba, T., Sakamoto, T., Koizumi, I., 2003.

Eastern Mediterranean surface water temperatures and $\delta^{18}O$ during deposition of sapropels in the late Quaternary. Paleoceanography 18, 1005. https://doi.org/10.1029/2000PA000617.
Engelhardt, J.F., Sudo, M., Stockhecke, M., Oberhänsli, R., 2017. Feldspar $^{40}Ar/^{39}Ar$ dating of ICDP PALEOVAN cores. Geochim. Cosmochim. Acta 217, 144–170.
Eshel, G., Farrell, B.F., 2000. Thermodynamics of Eastern Mediterranean Rainfall Variability. J. Atmos. Sci. 58, 88–92.
Francke, A., Wagner, B., Just, J., Leichner, N., Gromig, R., Baumgartnen, H., Vogel, H., Lacey, J.H., Sadori, L., Wonik, T., Leng, M.J., Zanchetta, G., Sulpizio, R., Giaccio, B., 2015. Sedimentological processes and environmental variability at Lake Ohrid (Macedonia, Albania) between 640 ka and present day. Biogeosci. Discuss. 12, 15111–15156.
Gagosian, R., Volkman, J.K., Nigrelli, G., 1983. The use of sediment traps to determine sterol sources in coastal sediments off Peru. In: Bjorøy, M., et al. (Eds.), Advances in Organic Geochemistry 1981. John Wiley & Sons Ltd., Chichester, pp. 369–379.
Gasse, F., Vidal, L., Develle, A.L., Van Campo, E., 2011. Hydrological variability in the Northern Levant: a 250 ka multiproxy record from the Yammouneh (Lebanon) sedimentary sequence, Clim. Past 7, 1261–1284.
Hodell, D., Crowhurst, S., Skinner, L., Tzedakis, P.C., Margari, V., Channell, J.E.T., Kamenov, G., Maclachlan, S., Rothwell, G., 2013. Response of Iberian Margin sediments to orbital and suborbital forcing over the past 420 ka. Paleoceanography 28 (1).
Hopmans, E.C., Sinninghe-Damsté, Schouten, S., 2016. The effect of improved chromatography on GDGT-based palaeoproxies. Org. Geochem. 93, 1–6.
Hopmans, E.C., Weijers, J.W.H., Schefuss, E., Herfort, L., Sinninghe-Damsté, J.S., Schouten, S., 2004. A novel proxy for terrestrial organic matter in sediments based on branched and isoprenoid tetraether lipids. Earth Planet. Sci. Lett. 224, 107–116.
Huguet, C., Hopmans, E.C., Febo-Ayala, W., Thompson, D.H., Sinninghe Damsté, J.S., Schouten, S., 2006. An improved method to determine the absolute abundance of glycerol dibiphytanyl glycerol tetraether lipids. Org. Geochem. 37, 1036–1041.
Huguet, C., Fietz, S., Moraleda, N., Litt, T., Heumann, G., Stockhecke, M., Anselmetti, F. S., Sturm, M., 2012. A seasonal cycle of terrestrial inputs in Lake Van, Turkey. Environ. Sci. Pollut. Res. 19, 3628–3635.
IAEA/WMO, 2014. Global Network of Isotopes in Precipitation, the GNIP Database, Erzurum, Turkey. IAEA Publ, Vienna.
Killops, S.D., Killops, V.J., 1997. Einführung in die Organische Geochemie. Enke Verlag, Stuttgart, 229 pp.
Kroon, D., Alexander, I., Little, M., Lourens, L.J., Matthewson, A., Robertson, A.H.F., Sakamoto, T., 1998. Oxygen isotope and sapropel stratigraphy in the Eastern Mediterranean during the last 3.2 million years. In: Proceedings of the ODP Scientific Results, pp. 181–190.
Kumar, D.M., Woltering, M., Hopmans, E.C., Sinninghe Damsté, J.S., Schouten, S., Werne, J.P., 2019. The vertical distribution of Thaumarchaeota in the water column of Lake Malawi inferred from core and intact polar tetraether lipids. Org. Geochem. 132, 37–49.
Kwiecien, O., Stockhecke, M., Pickarski, N., Heumann, G., Litt, T., Sturm, M., Anselmetti, F., Kipfer, R., Haug, G.H., 2014. Dynamics of the last four glacial terminations recorded in Lake Van, Turkey. Quat. Sci. Rev. 104, 42–52.
Lachner, J., Stockhecke, M., Beer, J., Christls, M., Heikkilä, U., 2021. Simultaneous ^{10}Be Variations in Polar Ice and Mid- Latitude Lake Sediment during Rapid Geomagnetic and Climatic Events (submitted).
Litt, T., Anselmetti, F.S., 2014. Lake Van deep drilling project PALEOVAN. Quat. Sci. Rev. 104, 1–7.
Litt, T., Ohlwein, C., Neumann, F.H., Hense, A., Stein, M., 2012. Holocene climate variability tn the Levant from Dead Sea pollen record. Quat. Sci. Rev. 49, 95–105.
Litt, T., Pickarski, N., Heumann, G., Stockhecke, M., Tzedakis, P.C., 2014. A 600,000 year long continental pollen record from Lake Van, eastern Anatolia (Turkey). Quat. Sci. Rev. 104, 30–41.
Loomis, S.E., Russell, J.M., Heureux, A.M., D'Andrea, W.J., Sinninghe Damsté, J.S., 2014. Seasonal variability of branched glycerol dialkyl glycerol tetraethers (brGDGTs) in a temperate lake system. Geochim. Cosmochim. Acta 144, 173–187.
Martínez-Sosa, P., Tierney, J.E., Meredith, L.K., 2020. Controlled lacustrine microcosms show a brGDGT response to environmental perturbations. Org. Geochem. 145, 104041.
Martrat, B., Grimalt, J.O., Lopez-Martinez, C., Cacho, I., Sierro, F.J., Abel Flores, J., Zahn, R., Canals, M., Curtis, J.H., Hodel, D.A., 2004. Abrupt temperature changes in the western Mediterranean over the past 250,000 years. Science 306, 1762–1765. https://doi.org/10.1126/science.1101706.
Miller, D.R., Habicht, M.H., Keisling, B.A., Castañeda, I.S., Bradley, R.S., 2018. A 900-year New England temperature reconstruction from in situ seasonally produced branched glycerol dialkyl glycerol teraethers (brGDGTs). Clim. Past 14, 1653–1667.
Naafs, B.D.A., Gallego-Sala, A.V., Inglis, G.N., Pancost, R.D., 2017. Refining the global branched glycerol dialkyl glycerol tetraether (brGDGT) soil temperature calibration. Org. Geochem. 106, 48–56.
North, S.M., Stockhecke, M., Tomonaga, Y., Mackay, A.W., 2017. Analysis of a fragmentary diatom record from Lake Van (Turkey) reveals substantial lake-level variability during previous interglacials MIS7 and MIS5e. J. Paleolimnol. https://doi.org/10.1007/s10933-017-9973-z.
Ozturk, F., Erkan, C., 2010. Bee Plants of Van Lake Basin (Turkey). Int. J. Bot. 6, 101–106.
Pickarski, N., Kwiecien, O., Langgut, D., Litt, T., 2015. Abrupt climate and vegetation variability of eastern Anatolia during the last glacial. Clim. Past 11, 1491–1505.
Randlett, M.-E., Coolen, M.J.L., Stockhecke, M., Pickarski, N., Litt, T., Balkema, C., Kwiecien, O., Tomonaga, Y., Wehrli, B., Schubert, C.J., 2014. Alkenone distribution in Lake Van sediment over the last 270 ka: influence of temperature and haptophyte species composition. Quat. Sci. Rev. 104, 53–62.
Randlett, M.-E., Bechtel, A., van der Meer, M.T.J., Peterse, F., Litt, T., Pickarski, N., Kwiecien, O., Stockhecke, M., Wehrli, B., Schubert, C.J., 2017. Biomarkers in Lake Van sediments reveal dry conditions in Eastern Anatolia during 110.000-10.000 years B.P. Geochem. Geophys. Geosyst. 18, 571–583.
Rasmusssen, S.O., Anderson, K.K., Svensson, A.M., Steffensen, J.P., Vinther, B.M., Clausen, H.B., Siggaard-Andersen, M.-L., Johnsen, S.J., Larsen, L.B., Dahl-Jensen, D., Bigler, M., Röthlisberger, R., Fischer, H., Goto-Azuma, K., Hansson, M.E., Ruth, U., 2006. A new Greenland ice core chronology fort he last glacial termination. J. Geophys. Res. 111 (D06102), 2006. https://doi.org/10.1029/2005JD006079.
Rodwell, M.J., Hoskins, B.J., 1996. Monsoons and the dynamics of deserts. Quart. J. Roy. Meteor. Soc. 122B, 1385–1404.
Rontani, J.F., Volkman, J.K., 2005. Lipid characterization of coastal hypersaline cyanobacterial mats from the Camargue (France). Org. Geochem. 36, 251–272.
Russell, J.M., Hopmans, E.C., Loomis, S.E., Liang, J., Sinninghe Damsté, J.S., 2018. Distributions of 5- and 6-methyl branched glycerol dialkyl glycerol tetraethers (brGDGTs) in East African lake sediment: effects of temperature, pH, and new lacustrine paleotemperature calibrations. Org. Geochem. 117, 56–69.
Sachse, D., Radke, J., Gleixner, G., 2006. δD values of individual *n*-alkanes from terrestrial plants along a climatic gradient—implications for the sedimentary biomarker record. Org. Geochem. 37, 469–483.
Sachse, D., Billault, I., Bowen, G.J., Chikaraishi, Y., Dawson, T.E., Feakins, S.J., Freeman, K.H., Magill, C.R., McInerney, F.A., van der Meer, M.T.J., Polissar, P., Robins, R.J., Sachs, J.P., Schmidt, H.-L., Sessions, A.L., White, J.W.C., West, J.B., Kahmen, A., 2012. Molecular Paleohydrology: interpreting the hydrogen-isotopic composition of lipid biomarkers from Photosynthesizing Organisms. Annu. Rev. Earth Planet. Sci. 40, 221–249.
Schouten, S., Hopmans, E.C., Schefuss, E., Sinninghe Damsté, J.S., 2002. Distributional variations in marine crenarchaeotal membrane lipids: a new tool for reconstructing ancient sea water temperatures? Earth Planet. Sci. Lett. 204, 265–274.
Sinninghe Damsté, J.S., Ossebaar, J., Abbas, B., Schouten, S., Verschuren, D., 2009. Fluxes and distribution of tetraether lipids in an equatorial African lake: constraints on the application of the TEX86 palaeothermometer and BIT index in lacustrine settings. Geochim. Cosmochim. Acta 73, 4232–4249.
Smith, F.A., Freeman, K.H., 2006. Influence of physiology and climate on δD of leaf wax *n*-alkanes from C_3 and C_4 grasses. Geochim. Cosmochim. Acta 70, 1172–1187.
Stockhecke, M., Anselmetti, F., Meydan, A.F., Odermatt, D., Sturm, M., 2012. The annual particle cycle in Lake Van (Turkey). Palaeogeogr. Palaeoclimatol. Palaeoecol. 333-334, 148–159.
Stockhecke, M., Kwiecien, O., Vigliotti, L., Anselmetti, F., Beer, J., Cağatay, M.-N., Channell, J.E.T., Kipfer, R., Lacher, J., Litt, T., Pickarski, N., Sturm, M., 2014a. Chronostratigraphy of the 600,000 year old continental record of Lake Van (Turkey). Quat. Sci. Rev. 104, 8–17.
Stockhecke, M., Sturm, M., Brunner, I., Schmincke, H.-U., Sumita, M., Kipfer, R., Kwiecien, O., Cukur, D., Anselmetti, F.S., 2014b. Sedimentary evolution and environmental history of Lake Van (Turkey) over the past 600,000 years. Sedimentology 61, 1830–1861.
Stockhecke, M., Timmermann, A., Kipfer, R., Haug, G.H., Kwiecien, O., Friedrich, T., Menviel, L., Litt, T., Pickarski, N., Anselmetti, F., 2016. Millennial to orbital-scale variations of drought intensity in the Eastern Mediterranean. Quat. Sci. Rev. 133, 77–95.
Svensson, A., Anderson, K.K., Bigler, M., Clausen, H.B., Dahl-Jensen, D., Davies, S.M., Johnsen, S.J., Muscheler, R., Parrenin, F., Rasmussen, S.O., Rothlisberger, R., Seierstad, I., Steffensen, J.P., Vinther, B.M., 2008. A 60,000 year Greenland stratigraphic ice core chronology. Clim. Past 4, 47–57.
Tierney, J.E., Russel, J.M., 2009. Distributions of branched GDGTs in a tropical lake system: implications for lacustrine application of the MBT/CBT paleoproxy. Org. Geochem. 40, 1032–1036.
Tierney, J.E., Russell, J.M., Eggermont, H., Hopmans, E.C., Verschuren, D., Sinninghe Damsté, J.S., 2010. Environmental controls on branched tetraether lipid distributions in tropical East African lake sediments. Geochim. Cosmochim. Acta 74, 4902–4918.
Tomonaga, Y., Brennwald, M.S., Livingstone, D.M., Kwiecien, O., Randlett, M.-E., Stockhecke, M., Unwin, K., Anselmetti, F.S., Beer, J., Haug, G.H., Schubert, C., Sturm, M., Kipfer, R., 2017. Porewater salinity reveals past lake-level changes in Lake Van, the Earth's largest soda lake. Sci. Rep. 7 (313), 1–10.
Tzerdakis, P.C., Hooghiemstra, H., Pälike, H., 2006. The last 1.35 million years at Tenaghi Philippon: revised chronostratigraphy and long-term vegetation trends. Quat. Sci. Rev. 25, 3416–3430.
van Bree, L.G.J., Peterse, F., Baxter, A.J., De Crop, W., van Grinsven, S., Villanueva, L., Verschuren, D., Sinninghe Damsté, J.S., 2020. Seasonal variability and sources of in situ brGDGT production in a permanently stratified African crater lake. Biogeosciences 17, 5443–5463.
van Zeist, W., Woldring, H., 1978. A postglacial pollen diagram from Lake Van in East Anatolia. Rev. Palaeobot. Palynol. 26, 249–276.
Vigliotti, L., Channell, J.E.T., Stockhecke, M., 2014. Paleomagnetism of Lake Van sediments: chronology and paleoenvironment since 350 ka. Quat. Sci. Rev. 104, 18–29.
Volkman, J.K., 2003. Sterols in microorganisms. Arch. Microbiol. Biotechnol. 60, 495–506.
Volkman, J.K., Barrett, S.M., Blackburn, S.I., Mansour, M.P., Sikes, E.L., Gelin, F., 1998. Microalgal biomarkers: a review of recent research developments. Org. Geochem. 29, 1163–1179.
Volkman, J.K., Barrett, S.M., Blackburn, S.I., 1999. Eustigmatophyte microalgae are potential sources of C_{29} sterols, C_{22}–C_{28} *n*-alcohols and C_{28}–C_{32} *n*-alkyl diols in freshwater environments. Org. Geochem. 30, 307–318.

Weber, Y., De Jonge, C., Rijpstra, W.I.C., Hopmans, E.C., Stadnitskaia, A., Schubert, C.J., Lehmann, M.F., Sinninghe Damsté, J.S., Niemann, H., 2015. Identification and carbon isotope composition of a novel branched GDGT isomer in lake sediments: evidence for lacustrine branched GDGT production. Geochim. Cosmochim. Acta 154, 118–129.

Weber, Y., Sinninghe Damsté, J.S., Zopfi, J., De Jonge, C., Gilli, A., Schubert, C.J., Lepori, F., Lehmann, M.F., Niemann, H., 2018. Redox-dependant niche differentiation provides evidence for multiple bacterial sources of glycerol tetraether lipids in lakes. PNAS 115, 10926–10931.

Wegwerth, A., Ganopolski, A., Ménot, G., Kaiser, J., Dellwig, O., Bard, E., Lamy, F., Arz, H.W., 2015. Black Sea temperature response to glacial millennial-scale climate variability. Geophys. Res. Lett. 42, 8147–8154. https://doi.org/10.1002/2015GL065499.

Weijers, J.W.H., Schouten, S., van den Donker, J.C., Hopmans, E.C., Sinninghe Damsté, J. S., 2007. Environmental controls on bacterial tetraether membrane lipid distribution in soils. Geochim. Cosmochim. Acta 71, 703–713.

West, J.B., Ehleringer, J.R., Cerling, T.E., 2007. Geography and vintage predicted by a novel GIS model of wine $\delta^{18}O$. J. Agric. Food Chem. 55, 7075–7083.

Wick, L., Lemke, G., Sturm, M., 2003. Evidence of Lateglacial and Holocene climatic change and human impact in eastern Anatolia: high-resolution pollen, charcoal, isotopic and geochemical records from the laminated sediments of Lake Van, Turkey. The Holocene 13, 665–675.